Study of Light Hypernuclei by Pionic Decay at JLab

N. Grigoryan, S. Knyazyan, A. Margaryan (*spokesperson*), G. Marikyan,
L. Parlakyan, S. Zhamkochyan, H. Vardanyan
Yerevan Physics Institute, 375036 Yerevan, Armenia

C. Chen, Liguang Tang (*spokesperson*), Z. Ye, L. Yuan (*spokesperson*)
Department of Physics, Hampton University, VA 23668, U.S.A.

O. Hashimoto (*spokesperson*), S.N. Nakamura (*spokesperson*)
Department of Physics, Tohoku University, Sendai, 98-77, Japan

J. Reinhold (*spokesperson*)
Department of Physics, Florida International University, Miami, FL , U.S.A.

Ed.V. Hungerford
Department of Physics, University of Houston, Houston, TX 77204, U.S.A.

S. Majewski
Thomas Jefferson National Accelerator Facility, Newport News, VA 23606, USA

B. Hu, J. Shen, W. Wang, X. Zhang, Y. Zhang
Nuclear Physics Institute, Lanzhou University, China

J. Feng, Y. Fu, J. Zhou, S. Zhou
Department of Physics, China Institute of Atomic Energy, China

Y. Jiang, H. Lu, X. Yan, Y. Ye
Department of Modern Physics, University of Science & Technology of China, China.

D. Androic, M. Furic, T. Petkovic, T. Seva
Department of Physics & Department of Applied Physics, University of Zagreb

Others to be confirmed

November 18, 2007

Abstract

We propose to investigate Λ hypernuclei in the A≤12 mass region by using decay pion spectroscopy. Binding energies and lifetimes of all separable hypernuclei or hyperfragments will be simultanuously measured with high precision. The project aims to determine precisely the binding energies of light hypernuclei, investigate production of exotic hypernuclei, and study impurity nuclear physics and the medium effect of baryons.

These investigations will fully utilize the unique parameters (high intensity, small emittance, and fine beam bunch time structure) of the CW electron beam at Jefferson Laboratory, and are enabled by the use of the high-resolution kaon spectrometer (HKS) in combination with a high-resolution magnetic spectrometer for hypernuclear decayed pions (*HπS* -Enge) in Hall C (or in Hall A). The experimental system is almost identical to the HKS (E01-011) experiment completed in 2005.

Ground state binding energy measurement for light hypernuclei must have a resolution better than σ=100 keV in order to separate possible doublets. For the proposed experiment, their absolute values will be determined with a precision better than 10 keV while the energy resolution will be σ≈55 keV.

The lifetimes of separatable hypernuclear states by π^--mesonic decays will be measured with accuracy of about 100 ps or better. Their values will be determined with precision of about 10 ps or better.

We propose to start by using existing spectrometers (HKS and Enge) and their detector packages, and two production targets ^7Li and ^{12}C.

1. Introduction

The binding energies of the Λ particle coupled to the nuclear core at ground state give one of the basic pieces of information on the Λ-nucleus interaction. Most of the observed hypernuclear decays take place from the ground states (or some of the long lived low lying states), because the electromagnetic interactions or Auger neutron emission process are generally faster than the weak decay of the Λ particle. The binding energy of Λ of a hypernucleus at ground state is defined by:

$$B_\Lambda(g.s.) = M_{core} + M_\Lambda - M_{HY}.$$

The mass M_{core} is merely the mass of the nucleus that is left in the ground state after the Λ particle is removed. The M_Λ and M_{HY} are the masses of Λ and ground state hypernucleus, respectively. The binding energies, B_Λ, have been measured in emulsion for a wide range of light ($3 \leq A \leq 15$) hypernuclei [1]. These have been made exclusively from the unique weak π^--mesonic decay of Λ. The precise values of the binding energies of Λ in the few-baryon systems provide filters through which one can look at particular aspects of the *YN* interaction, and one of the primary goals in hypernuclear physics is to extract information about *YN* interactions through precise calculations of few-body systems such as $^3_\Lambda H$, $^4_\Lambda H$, and $^4_\Lambda He$. The existing situation can be summarized by the help of words from R. Dalitz [2]:

"$^3_\Lambda H$ was well known very early and has been studied a great deal. Its B_Λ value is quite small and difficult to measure. It was the first hypernucleus to be considered a "Λ halo". The value of 0.13±0.05 MeV by Don Devis [1] quoted above was from emulsion studies. From HeBC studies, Keyes et al. [3] have given 0.25±0.31 MeV for all events ($^3He\pi^-$) but got -0.07±0.27 when they added in all other π^- modes, which is not reassuring. For $R_3 = n(^3He\pi^-)/n(^3H\pi^- \rightarrow$ all π^- modes) they gave $R_3 = 0.36±0.07$, and consider this to correspond to $0.11^{+0.06}_{-0.03}$ MeV for its B_Λ value, I feel that we are far from seeing the end of this road. A good deal of theoretical work on this 3-body system would still be well justified."

In addition, a rich amount of physics associated with the new degree of freedom brought by Λ particle into the nuclear medium can be offered by the weakly decayed pions from various parent hypernuclear species as we will discuss in detail in the next chapter. However, in the past energy resolution and precision (systematic error) have always been the problem in gaining precisely needed information because of the low energy of the decay pions. High precision energy calibration to reduce systematic errors was difficult for emulsion and He bubble chamber (*HeBC*) besides very low statistics. In modern counter type of experiments using mesonic beams (such as pions and kaons), thick targets which were used to compensate the low beam intensity caused problems in poor resolution and precision of the order of a few MeV. High statistics and thin targets can be achieved by the FINUDA experiment using an e^+e^- collider to produce Φ mesons at rest, but the detector system cannot provide a resolution better than 2 MeV for the decay pions with momentum of about 100 MeV/c.

Recent accomplishment of high precision γ-spectroscopy experiments with resolution in the order of a few keV have demonstrated the power of studying the transitions from the electromagnetic decay of selectively excited hypernuclear states by the (K, π) or (π, K)

reactions. However, as D.J. Millener pointed out in his presentation at the 2007 fall DNP meeting, γ-spectroscopy cannot provide information about the B_Λ of the ground states besides the limitation of selectivity on specific excited states.

Therefore, pionic decay spectroscopy with high energy resolution and precision in terms of binding energy determination and good statistics is highly attractive and needed. We propose a new experiment for precise measurement of the decay pions on their momenta and decay time for a light (A $\leq$ 12) mass range of hypernuclei (ordinary or exotic, produced either directly or indirectly through the process of fragmentations) at CEBAF. Binding energies B_Λ and lifetimes on various hypernuclear species (ground states and separable low lying states) can be simultaneously obtained. JLAB is the unique and only facility to establish such a program because of the following reasons:

(1) High precision beam provides point reaction position on target;
(2) High intensity, 100% duty factor, and excellent kaon spectrometer (HKS) with large solid angle acceptance at small forward scattering angle besides its high momentum resolution (2×10^{-4}) and short path length, allow to use extremely thick target to minimize the target loss uncertainty because of high production yield of hypernuclei;
(3) Because of high yield a high resolution low momentum spectrometer with reasonably large solid angle acceptance can be used to study the decay pions with high energy resolution of ~55 keV rms, sufficient to isolate states separated by ~120 keV or larger;
(4) Excellent calibration tool using elementary production of Λ particle can ensure a binding energy precision at the level of 10 keV; and
(5) Precise beam structure and excellent production and decay time reconstruction capability from the high resolution spectrometers make possible to measure lifetimes for all isolatable hypernuclear states with a precision in the order of ~10 ps for both statistical and systematic errors.

Wide range of physics (to be discussed in the next chapter) can be studied from single experiment, such as precise B_Λ for ground states and low lying states of ordinary hypernuclei, investigation of exotic hypernuclei toward neutron and proton drip-lines, study of impurity nuclear physics (low lying nuclear structure and glue-like role of Λ particle, and the medium effect of baryons.

We propose to carry out an experiment for these investigations by using the existing HKS+Splitter system and a HπS magnetic spectrometer (existing Enge spectrometer) in Hall C (or Hall A) with thin ^{12}C and ^{7}Li targets.

2. Physics Subjects

The physics subjects which can be pursued by precision hypernuclear spectroscopy are enlightening in particular in the current projects [5, 6] (see also [7-12]). The physics subjects which can be specifically studied but not limited by precise decay pion spectroscopy can be summarized as:

1) YN interactions,
2) Study of exotic hypernuclei,
3) Impurity nuclear physics, and
4) Medium effect of baryons- B(M1) measurement.

2.1 YN interaction

From precise binding energy B_Λ of hypernuclear ground states and detailed low lying structure, we can establish the ΛN spin-dependent (spin-spin, spin-orbit, and tensor forces) interaction strengths, investigate ΣN-ΛN coupling force, and study charge symmetry breaking. Experimental information on these characteristics of the ΛN interaction plays an essential role to discriminate and improve baryon-baryon interaction models, not only those based on the meson-exchange picture but also those including quark-gluon degree of freedom, toward unified understanding of the baryon-baryon interactions. In addition, understanding of the YN and YY interactions is necessary to describe high density nuclear matter containing hyperons.

The binding energies of the ground state of light hypernuclei are the most valuable experimental information for checking different models of YN interaction. Table 1 taken from reference [12] lists the results of the Λ separation energies obtained as a result of ab initio calculations using YN interactions with an explicit Σ admixture. Experimental results from emulsion are listed as comparison and additional systematic error in the order of about 40 keV is not included. It is demonstrated that for future theoretical developments more precise experimental measurements for binding energies are needed. The precision of the proposed experiment can put further stringent limit on the theoretical models.

Table 1: Λ separation energies, given in units of MeV, of A = 3-5 Λ hypernuclei for different models of YN interaction.

YN	$B_\Lambda(^3_\Lambda H)$	$B_\Lambda(^4_\Lambda H)$	$B_\Lambda(^4_\Lambda H^*)$	$B_\Lambda(^4_\Lambda He)$	$B_\Lambda(^4_\Lambda He^*)$	$B_\Lambda(^5_\Lambda He)$
SC97d(S)	0.01	1.67	1.2	1.62	1.17	3.17
SC97e(S)	0.10	2.06	0.92	2.02	0.90	2.75
SC97f(S)	0.18	2.16	0.63	2.11	0.62	2.10
SC89(S)	0.37	2.55	Unbound	2.47	Unbound	0.35
Experiment	0.13 ± 0.05	2.04 ± 0.04	1.00 ± 0.04	2.39 ± 0.03	1.24 ± 0.04	3.12± 0.02

In addition, with high precision and resolution the π^- decay can be used as effective tool to obtain spectroscopic information on hypernuclear structure, due to the selective character and sensitive shell-structure dependence [13, 14].

2.2 Study of exotic hypernuclei

There is currently in the nuclear physics community a strong interest in the study of nuclei very far from the valley of stability. It would allow one to apprehend the behavior of nuclear matter under extreme conditions. Hypernuclei can be even better candidates than ordinary nuclei to study nuclear matter with extreme N/Z ratios because more extended mass distributions are expected than in ordinary nuclei thanks to the glue-like role of the Λ due to the short range interaction nature by missing *OPE* force, and its effect on neutron halo [15] (such as the case of $^7_\Lambda He$). In Table 2 (see in later Chapter), especially, we see many particle

stable hypernuclei with unstable nuclear cores: $^6_\Lambda He$, $^7_\Lambda Be$, $^8_\Lambda He$, $^9_\Lambda Be$. Other exotic hypernuclei with neutron excess may exit: e.g. $^6_\Lambda H$, $^7_\Lambda H$, $^8_\Lambda H$, $^{10}_\Lambda He$, $^{11}_\Lambda Li$ (see also [16, 17]). These hypernuclei and other exotic hypernuclei with neutron and proton excess are expected to be photo-produced indirectly through the process of fragmentation – hyperfragments - from heavier targets and their two-body pionic decays can be detected by *HπS*.

2.3 Impurity nuclear physics

Since hyperons are free from the Pauli effect and feel nuclear forces different from those nucleons do in a nucleus, a hyperon introduced in a nucleus may give rise to various changes of the nuclear structure, such as changes of the size and the shape, change of the cluster structure, emergence of new symmetries, change of collective motions, etc. A beautiful example of how we may modify a nucleus by adding to it a distinguishable baryon in a well defined state is given by the experiment on γ-spectroscopy of $^7_\Lambda Li$. $^7_\Lambda Li$ is produced by means of the reaction $\pi^+ + {^7Li} \rightarrow {^7_\Lambda Li} + K^+$ at 1.05 GeV/c using the SKS spectrometer at KEK. $^7_\Lambda Li$ may be formed in the ground or low lying excited states. When a Λ in a 1s orbit is added to a loosely bound nucleus such as ^6Li, the nucleus is expected to shrink into a more compact system due to the attractive force between Λ and nucleons ("glue-like" role of the Λ) which results from the property of the Λ of being free from the Pauli blocking in a nucleus. This effect can be verified from the E2 transition probability B(E2), which contains information of the nuclear size. The E2 ($5/2^+ \rightarrow 1/2^+$) transition of $^7_\Lambda Li$ is essentially the E2 ($3^+ \rightarrow 1^+$) transition of the core nucleus ^6Li, but the existence of a Λ in the 1s orbit is expected to shrink the ^6Li core. Experimentally, B(E2) is derived from the lifetime of the $5/2^+$ state. The expected lifetime ($\sim 10^{-11}$ sec) is of the same order of the stopping time of the recoil $^7_\Lambda Li$ in lithium in the case of the (π^+, K^+) reaction at 1.05 GeV/c and was derived to be $5.8^{+0.9}_{-0.7} \pm 0.7$ ps with the Doppler shift attenuation method (DSAM). B(E2) was then derived to be $3.6 \pm 0.5^{+0.5}_{-0.4}$ e^2fm^4. This result, compared with the B(E2) = 10.9 ± 0.9 e^2fm^4 of the core nucleus ^6Li ($3^+ \rightarrow 1^+$), indicates a shrinkage of the $^7_\Lambda Li$ size from ^6Li by about 20% [18, 19].

The Doppler shift attenuation method (DSAM) can be applied to measure lifetimes in the range of $10^{-12} - 10^{-11}$sec, as in the B(E2) measurement of $^7_\Lambda Li$. For the M1 transition with energy about or less than 0.1 MeV and the E2 transition with energy around 1 MeV the expected lifetimes will be too long ($\sim 10^{-10}$sec) for DSAM and the γ transition competes with weak decay. Thus a new "γ-weak coincidence method" has been proposed [20] for the future J-PARC experiment.

This method is to determine the transition probability from the total decay rate (λ_B) of the upper state B (see in Fig. 1) and branching ratio (m) of the γ decay. The lifetime of B is directly measured from the time difference of hypernuclear production and emission of weak-decay particles (p and π^-). If γ transitions to populate B state from upper states (such as C) are much faster than the total decay rate of B(λ_B), as is usually the case for a small ground doublet spacing, the time spectrum of weak decay particles measured in coincidence with the B $\rightarrow$ Aγ ray is expressed as:

$$P^{B \to A}(t) = \frac{\lambda_A \lambda_B}{\lambda_A - \lambda_B} m N_B (e^{-\lambda_A t} - e^{-\lambda_B t}),$$

where λ_A denotes the decay rate of A and N_B denotes the initial population of the state B (including C→B). From this growth-decay function, λ_A and λ_B can be determined.

When the B→A transition is much slower than the weak decay, λ_B is determined from the time spectrum of weak decay particles in coincidence with C→B γ rays, which is expressed as:

$$P^{C \to B}(t) = \lambda_B N_B^{C \to B}[(1 - m\frac{\lambda_B}{\lambda_B - \lambda_A})e^{-\lambda_B t} + m\frac{\lambda_A}{\lambda_B - \lambda_A}e^{-\lambda_A t}].$$

Here, $N_B^{C \to B}$ is the population of B via the fast C→B transition. In general by measuring both $P^{B \to A}(t)$ and $P^{C \to B}(t)$, and fitting them to the equations above, λ_B can be determined precisely in a wide range. The branching ratio m of the B→A transition is measured from the γ-ray yield of B→A transition in coincidence with the C→B transition.
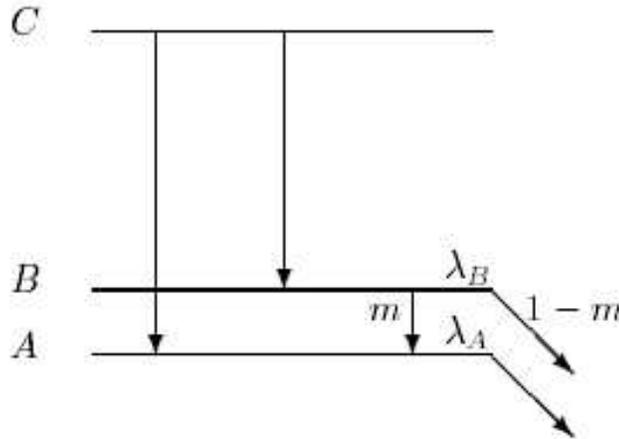

Figure 1: Method of B(E2) and B(M1) measurement from coincidence events of γ-ray and weak-decay particles.

In our case the high momentum resolution and high time resolution of $H\pi S$ allow us to separate pionic decays from the A and B states (see e.g. in Fig. 2) and to measure precisely the weak decay time spectra $P^{B \to weak}(t)$ and $P^{A \to weak}(t)$ separately. The time spectrum of weak-decay pions from the B state is:

$$P^{B \to weak}(t) = (1 - m)\lambda_B N_B e^{-\lambda_B t},$$

while the time spectrum of weak-decay pions from A state is:

$$P^{A \to weak}(t) = P^{B \to A}(t) + \lambda_A N_A e^{-\lambda_A t},$$

7

where N_A denotes the initial population of the state A (including C→A). By measuring both of $P^{B→weak}(t)$ and $P^{A→weak}(t)$ and fitting them together to the equations above, λ_A, λ_B, and m can be determined precisely. In general, it is assumed that the weak decay rates of A and B states are the same, i.e. $\lambda_A = \lambda_W$, $\dfrac{1}{\lambda_B} = \dfrac{1}{\lambda_W} + \dfrac{1}{\lambda_\gamma}$ and $m = \dfrac{\Gamma_\gamma}{\Gamma_\gamma + \Gamma_w} = \dfrac{\lambda_w}{\lambda_\gamma + \lambda_w}$. We call it the "tagged-weak pi-method". With the precision of our experiment, it can be used for investigating the E2 or M1 transitions with lifetimes in the range of about 50-400 ps. Therefore, our experiment will provide complementary results to the "γ-weak coincidence" experiment at J-PARC and may have significant advantages on some hypernuclei.

2.4 Medium effect of baryons – B(M1) measurement

Using hyperons free from the Pauli effect, we can investigate possible modification of baryons in nuclear matter through magnetic moments of hyperons in a nucleus. Magnetic moments of baryons can be well described by the picture of constituent quark models in which each constituent quark has a magnetic moment of a Dirac particle having a constituent quark mass. If the mass (or the size) of a baryon is changed in a nucleus by possible partial restoration of chiral symmetry, the magnetic moment of the baryon may be changed in a nucleus. A Λ particle in a hypernucleus is the best probe to see whether such an effect really exists or not. Here we propose to derive a g-factor of Λ in the nucleus from a probability (B(M1) value) of a spin-flip M1 transition between hypernuclear spin-doublet states. In the weak coupling limit between a Λ and a core nucleus, the B(M1) is expressed as [21]:

$$B(M1) \propto \left| \left\langle \phi_{lo} \left| \mu^z \right| \phi_{up} \right\rangle \right|^2 = \left| \left\langle \phi_{lo} \left| g_N J_N^z + g_\Lambda J_\Lambda^z \right| \phi_{up} \right\rangle \right|^2 \propto (g_N - g_\Lambda)^2,$$

where g_N and g_Λ denote effective g-factors of the core nucleus and the Λ, and J_N^z and J_Λ^z denote their spin operators, respectively. Here the space components of the wave functions of the lower and upper states of the doublet (ϕ_{lo}, ϕ_{up}) are assumed to be identical.

Transition probabilities such as B(M1) are derived from lifetimes of low lying excited states, using the "Doppler shift attenuation method" or "γ-weak coincidence method" [7, 8, 20]. We propose to use "tagged-weak pi-method" in our experiment.

3. Previous Experiments and Current Projects

Λ hyperon separation energies B_Λ have been measured in emulsion for a wide range of light ($3 \le A \le 15$) hypernuclei. The kinematical analysis of the decayed fragments in nuclear emulsion in the past was the best method for determining the binding energy of the Λ particle in the hypernucleus. These have been made exclusively from π⁻-mesonic decays. Identification was established if one, and only one, energy and momentum balance was obtained after permuting all possible identities of the nuclear decay particles. The emulsion data on B_Λ values, culled from some 36000 π⁻-mesonic decaying hypernuclei produced by stopping K⁻ mesons [1, 23], are summarized in Table 2. This compilation included 4042 uniquely identified events.

Table 2: Λ binding energies B_Λ (MeV) of light hypernuclei measured in emulsion. In addition to the quoted statistical errors, there are systematic errors of about 0.04 MeV. Calculated corresponding decay pion momentum and number of observed events are presented as well.

Hypernucleus	B_Λ (MeV)	Decay π^- momentum (MeV/c)	Number of events
$^3_\Lambda H$	0.13 ± 0.05	114.3	204
$^4_\Lambda H$	2.04 ± 0.04	132.9	155
$^4_\Lambda He$	2.39 ± 0.03	97.97	279
$^5_\Lambda He$	3.12 ± 0.02	99.14	1784
$^6_\Lambda He$	4.18 ± 0.1	108.4	31
$^7_\Lambda He$	Not averaged 5.44-expected	115.1 (expected)	16
$^7_\Lambda Li$	5.58 ± 0.03	107.9	226
$^7_\Lambda Be$	5.16 ± 0.08	95.8	35
$^8_\Lambda He$	7.16 ± 0.7	116.3	6
$^8_\Lambda Li$	6.80 ± 0.03	124.1	787
$^8_\Lambda Be$	6.84 ± 0.05	97.17	68
$^9_\Lambda Li$	8.53 ± 0.15	121.1	8
$^9_\Lambda Be$	6.71 ± 0.04	95.96	222
$^9_\Lambda B$	8.29 ± 0.18	96.72	4
$^{10}_\Lambda Be$	9.11 ± 0.22	104.3	1
$^{10}_\Lambda B$	8.89 ± 0.12	100.5	10
$^{11}_\Lambda B$	10 .24 ± 0.05	105.9	73
$^{12}_\Lambda B$	11 .37 ± 0.06	115.8	87

The results of the compilation are illustrated also in Fig. 2 giving the B_Λ distributions for all the hypernuclear species, from which it follows that the binding energy resolutions in emulsion lies in the range 0.5-1.0 MeV.

As mentioned earlier, from HeBC studies, Keyes et al. [3] have given From HeBC studies, Keyes et al. [3] have given $B_\Lambda(^3_\Lambda H) = 0.25 \pm 0.31$ MeV for all events ($^3He\pi^-$) but got $B_\Lambda(^3_\Lambda H) = -0.07 \pm 0.27$ MeV when they added in all other π^- modes.

The Λ binding energies for some light hypernuclei were also measured by reactional mass spectroscopy using the (π^+, K^+) reaction (see e.g. the review paper of Hashimoto and Tamura [8]) and are summarized in Table 3, where the corresponding emulsion data are presented as well for comparison.
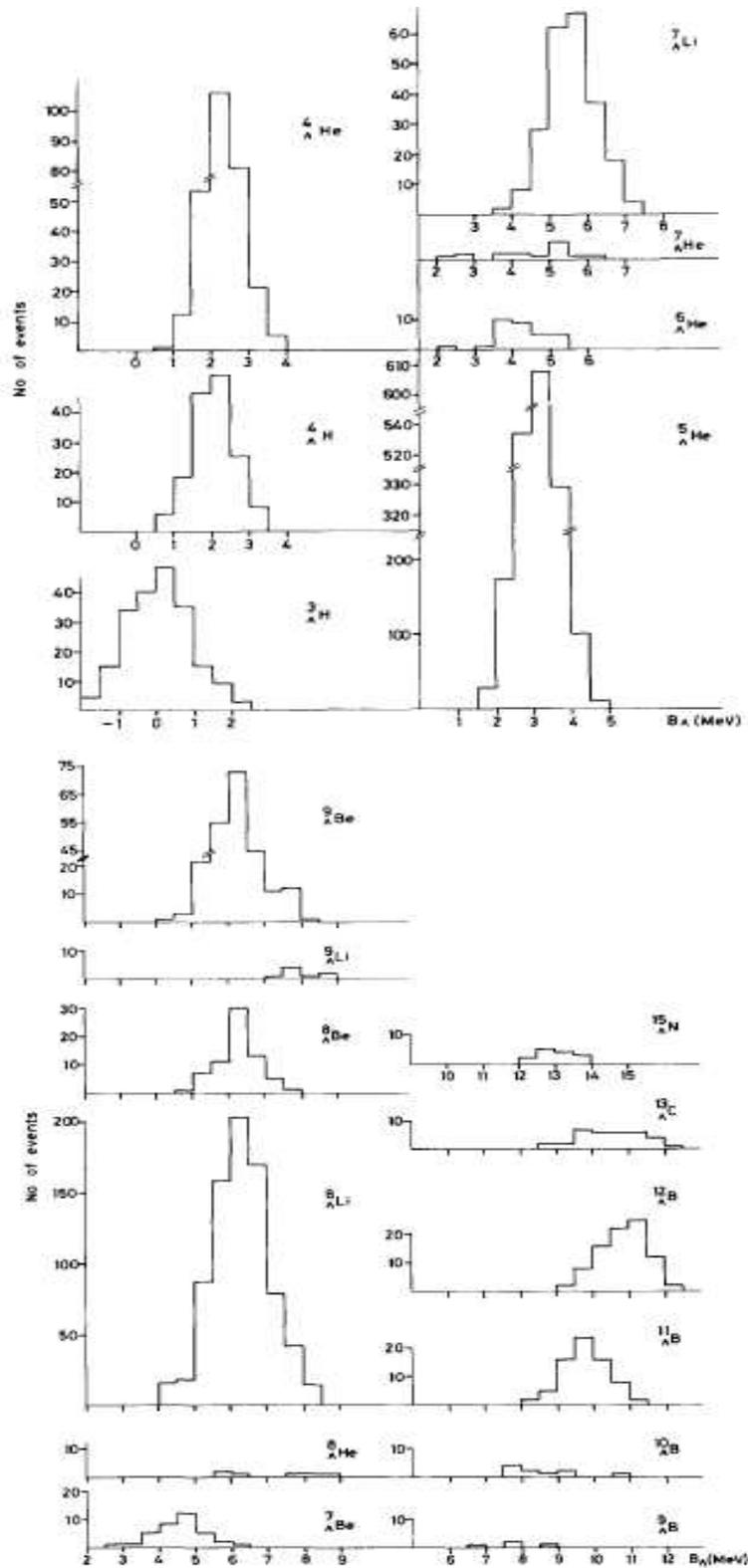
Figure 2: Distributions of the B_Λ values for the hypernuclei of mass number A ≤ 15. Figure is taken from reference [23].

Table 3: Λ binding energies B_Λ (MeV) of light hypernuclei measured in emulsion and in (π^+, K^+) reaction spectroscopy. In addition to the quoted statistical errors, there is a systematic error of about 0.36 MeV in the (π^+, K^+) reaction data.

Hypernuclide	B_Λ (MeV) emulsion	B_Λ (MeV) (π^+, K^+) reaction spectroscopy
$^7_\Lambda Li$	5.58 ± 0.03	5.22 ± 0.08
$^9_\Lambda Be$	6.71 ± 0.04	5.99 ± 0.07
$^{10}_\Lambda B$	8.89 ± 0.12	8.1 ± 0.1
$^{12}_\Lambda C$	10.76 ± 0.19	10.8 (Adjusted)
$^{13}_\Lambda C$	11.69 ± 0.12	11.38 ± 0.05

The absolute mass scales of (π^+, K^+) reaction spectroscopy have been adjusted (or aligned) using as a reference the $^{12}_\Lambda C$ ground-state peak, whose binding energy is believed to be well determined from the emulsion experiments to be 10.76 MeV. Considering the fact that the binding energies of $^7_\Lambda Li$ and $^{13}_\Lambda C$ agree reasonably with the emulsion data within the overall experimental errors, the differences in case of $^9_\Lambda Be$ and $^{10}_\Lambda B$ are significant even if we include the systematic errors. The reason for this disagreement is not known. These results and current theoretical investigations indicate the necessity and importance of new and precise measurement of the B_Λ values of light hypernuclei.
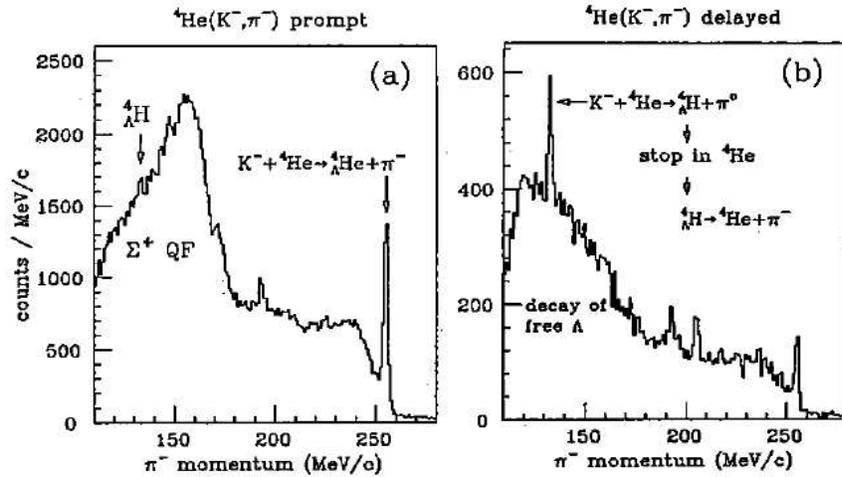

Figure 3: Time gated momentum spectra of π^- from K^- absorption at rest on ^4He target (from Ref. [25]. The $^4_\Lambda H$ peak is enhanced in the spectrum for delayed events: (a) $t_{react.} \leq 0.3$ ns (prompt events); b) $0.3 \leq t_{react.} \leq 1.5$ ns (delayed events).

The hypernuclear decayed discrete π^- spectra can be measured by using a magnetic spectrometer, but in conventional fixed target experiments employing mesonic beams, the need to use thick targets to gain yield rate introduces major limitations on the achievable resolution. The low yield prevents also the usage of spectrometer for decayed pions due to

smaller solid anagle acceptance. The momentum resolution of the Tokyo group's magnetic spectrometer e.g. was ~1 MeV [24]. Nevertheless, the Tokyo group was the first to detect the decayed discrete π^- mesons from $^4_\Lambda H$ hyperfragments as a "*delayed-particle*" in the stopped K^- reactions by a magnetic spectrometer (see Fig. 3 taken from Ref. [25]). This result is a clear demonstration for a new hypernuclear spectroscopy by the π^- decay.

The ongoing FINUDA experiment studies hypernuclei produced also by the stopped K^- reaction. Due to high low energy K^- production and stop rates, thin targets are allowed to be used. However, the momentum resolution of the FINUDA spectrometer [26] is about 2 MeV in the 100 MeV/c range. The proposed Cylindrical Detector System at J-PARC [7] is also about the same as that from FINUDA.

Therefore, the decay π^- study is highly interesting because it offers a rich amount of physics. However, resolution and precision are the keys to be successful.

4. Production of Hypernuclei

Any process which is capable of producing a Λ hyperon, may, when occurring in a nucleus, produce a hypernucleus. Two main mechanisms exist for hypernuclear formation, direct and indirect.

4.1 Direct production mechanism

Various Λ hypernuclear states can be directly populated by means of different reactions. The larger amount of data has been produced so far by means of the strangeness exchange two-body reaction: $K^- n \rightarrow \Lambda \pi^-$ on a neutron of a nucleus with K^- at rest and in flight. Recently, the associated production reactions, $\pi^+ n \rightarrow \Lambda K^+$ and $e p \rightarrow e' \Lambda K^+$, were also proved to be very efficient for producing Λ-hypernuclei at KEK and JLAB, respectively. The photon energy dependence of the elementary cross sections for the six isospin channels of kaon photo-production is shown in Fig. 4, taken from reference [27]. The cross section for the $\gamma p \rightarrow \Lambda K^+$ reaction rises sharply at the threshold energy Eγ = 0.911 GeV and stays almost constant from 1.1 to 1.6 GeV. From Fig. 4, it follows that in case of the photo-nuclear reaction, we have three sources for K^+ mesons, with approximately equal weights. However, only the reaction $\gamma p \rightarrow \Lambda K^+$ is associated to the direct population of hypernuclear states.

The differential cross section of the $\gamma p \rightarrow \Lambda K^+$ reaction taken from [26] is shown in Fig. 5. From Fig. 5, it follows that at forward direction $d\sigma/d\Omega$ (0°, $\gamma p \rightarrow \Lambda K^+$) ≈ 0.35 $\mu b/sr$. The quasi-free kaon production cross section on the nucleus can be assumed to scale as Z$^{0.8}$[28] and for the differential cross section of the $^{12}C(\gamma, K^+)$ reaction we have about $d\sigma/d\Omega$ (0°, γ $^{12}C \rightarrow K^+ + X$) $\approx 4.2 \times 0.35 = 1.47$ $\mu b/sr$.
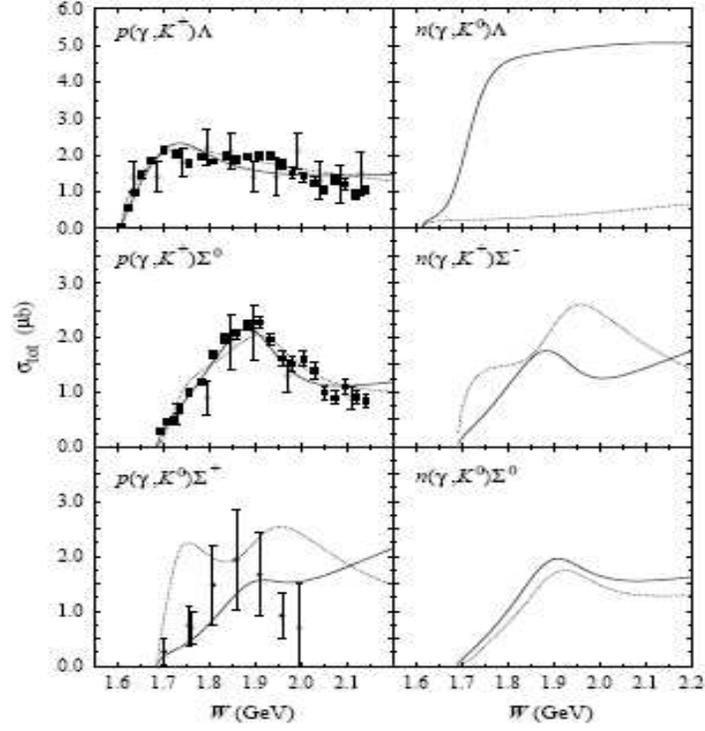
Figure 4: Total cross sections for the six isospin channels of kaon photoproduction on nucleon (from [27]).
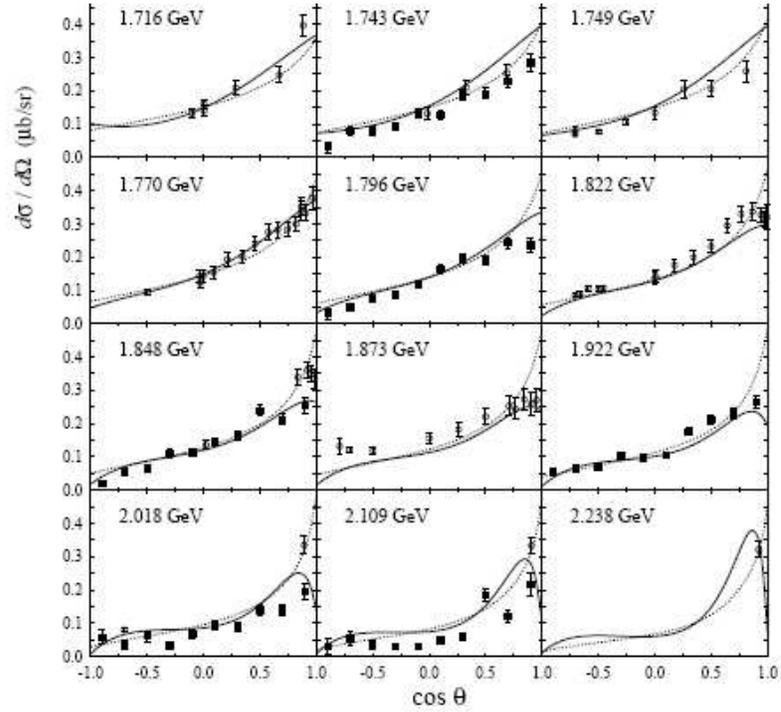

Figure 5: Differential cross section for $p(\gamma, K^+)$ channel. The total c.m. energy W is shown in every panel (for details see [27]).

The cross sections of the hypernuclear states for the targets ^7Li and ^{12}C have been calculated by Motoba and Sotona for the forward produced K^+ mesons [5, 29] (as well as measured with good agreement by the JLAB experiments in Hall C – HNSS and HKS). They are listed in Table 4. The angular distribution of kaons in the $^{12}C(e, e'K^+)^{12}_\Lambda B$ reaction is displayed in Fig. 6. As shown in Fig. 6, the angular distribution of kaons is forward peaked. From this distribution one can estimate that the total cross section is about σ_t ($^{12}C(e, e'K^+)^{12}_\Lambda B) = \int(d\sigma/d\Omega)d\Omega \approx 31$ nb.

Table 4: Cross section $d\sigma/d\Omega(\theta = 0°, \gamma + {}^AZ \to {}^A_\Lambda(Z-1) + K^+$ calculated by DWIA (from [5]).

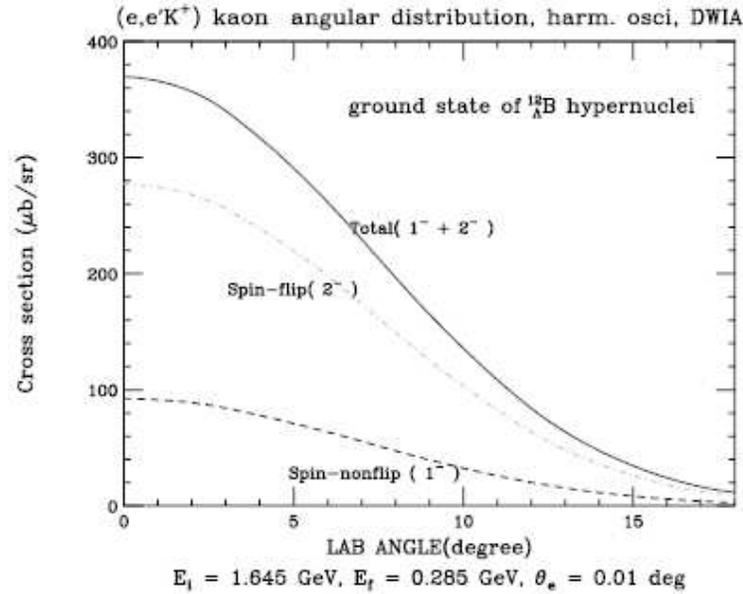| Target	Hypernucleus	Hypernuclear configuration	Cross section (nb/sr)
^7Li	$^7_\Lambda He$	$s_{1/2}$	28
		$s_{1/2}$	11
		$p_{3/2}$	15
		$s_{1/2}$	52
^{12}C	$^{12}_\Lambda B$	$s_{1/2}$	112
		$p_{3/2}$	79
		$p_{1/2}$	45

Figure 6: Angular distribution of kaon in the $^{12}C(e, e'K^+)^{12}_\Lambda B$ reaction (taken from Ref. [5]).

However, for kaons produced in the forward direction the probability of bound $^{12}_{\Lambda}B^*$ population or the Λ sticking probability, which is equal to the ratio of the corresponding differential cross sections, is quite high and for zero angle amounts: $0.36/1.47 = 0.24$. We assume that in the angular range from 0° to 15° the quasi-free produced kaons are distributed uniformly. In such a condition, the average cross section of the $^{12}C(e,e'K^+)^{12}_{\Lambda}B^*$ reaction is: $\overline{d\sigma/d\Omega(\gamma+{}^{12}C\rightarrow{}^{12}_{\Lambda}B^* + K^+)} \cong 170$ nb/sr (agreed reasonably well with the results from Hall C experiments) and the average probability of $^{12}_{\Lambda}B^*$ population, triggered by kaons detected in the 0° to 15° angular range, is equal to the ratio $0.17/1.47 \cong 0.11$. Consequently, in the same conditions the average cross section of the $^7Li(e,e'K^+)^7_{\Lambda}He^*$ reaction is: $\overline{d\sigma/d\Omega(\gamma+{}^7Li\rightarrow{}^7_{\Lambda}He^* + K^+)} \cong 76.5$ nb/sr. These cross sections can be used to estimate yields of directly produced $^{12}_{\Lambda}B^*$ and $^7_{\Lambda}He^*$ hypernuclei in coincidence with forward produced kaons detected in HKS.

4.2 Indirect production mechanism

On the other hand, it is known from old emulsion experiments [1] that various hypernuclei, including proton or neutron rich ones, can be produced as hyperfragments by K^- induced reactions (see previous Table 2). Formation probabilities of $^4_{\Lambda}H$ hypernuclei in the K^- absorption at rest on ^4He, ^7Li, ^9Be, ^{12}C, ^{16}O, and ^{40}Ca targets have been measured with the aid of the characteristic π^- (133 MeV/c) from the two-body decay of $^4_{\Lambda}H$, $(^4_{\Lambda}H \rightarrow {}^4He +\pi^-)$, at KEK [33] as well. The production rates $^4_{\Lambda}H$ obtained by the KEK group [33] and by the European K^- Collaboration [1] are shown in Table 6. Similarly, the rates of production of $^3_{\Lambda}H$ and $^5_{\Lambda}He$ by stopping K^- mesons have been deduced [1] and are given in Table 7.

Table 6: Comparison of $^4_{\Lambda}H$ production rates by stopping K⁻ mesons.

KEK (Tokyo)		European K⁻ Collaboration	
Target	Rate ($\times10^{-3}$)	Target	Rate ($\times10^{-3}$)
^7Li	30		
^9Be	15.7		
^{12}C	10.0	C, N, O	7.3
^{16}O	4.7		
^{40}Ca	≤ 2.7	Ag, Br	2.4

Table 7: Production rates of $^3_{\Lambda}H$ and $^5_{\Lambda}He$ measured by the European K^- collaboration.

Target	$^3_{\Lambda}H$ rate ($\times10^{-3}$)	$^5_{\Lambda}He$ ($\times10^{-3}$)
C, N, O	1.62	21.6
Ag, Br	0.54	1.4

It is to be noticed that the $^4_\Lambda H/^3_\Lambda H$ production ratio is ≈ 5 for both light and heavy targets. The large drop in $^5_\Lambda He$ production in going from light to heavy targets is explained by the strong inhibtion of helium emission due to the high Coulomb barrier presented by silver and bromine nuclei.

From observations of neutral hyperon emission it has been shown that the overall hypernuclear production rates by stopping K^- mesons are $8 \pm 2\%$ from C, N, O and $58 \pm 15\%$ from Ag, Br.

The two body reactions for K^- absorption at rest, which produce strangeness (which finally results in a Λ hyperon) in the nucleus, are listed in Table 8.

Table 8: Two body reactions that produce strangeness (Λ hyperon) by K^- absorption at rest.

$K^- + p \rightarrow \Lambda + \pi^0$	$K^- + n \rightarrow \Lambda + \pi^-$
$K^- + p \rightarrow \Sigma^- + \pi^+$	$K^- + n \rightarrow \Sigma^- + \pi^0$
$K^- + p \rightarrow \Sigma^0 + \pi^0$	$K^- + n \rightarrow \Sigma^0 + \pi^-$
$K^- + p \rightarrow \Sigma^+ + \pi^-$	

The observed formation probabilities of hyperfragments per stopped K^- could be explained by a model in which a quasi-free produced Λ is trapped in the nucleus and forms a "Λ compound nucleus", which may decay into a hyperfragment such as $^4_\Lambda H$. In this model, which was proposed by Tamura et al. [34], the $^4_\Lambda H$ formation probabilities per produced Λ can be expressed in terms of three physical factors as:

$$P(^4_\Lambda H) = \int P_\Lambda (E_\Lambda) F_C (E_\Lambda) D_C (^4_\Lambda H, E_X) dE_\Lambda \, ,$$

where, $P(E_\Lambda)$ represents the energy distribution of produced Λ. $F_C(E_\Lambda)$ stands for the formation probability of a Λ compound nucleus, when a Λ with a kinetic energy E_Λ is produced. $D_C(^4_\Lambda H, E_X)$ is the probability of forming $^4_\Lambda H$ from the Λ compound nucleus with excitation energy E_X. The calculated values in the case of stopped K^- are shown in the Fig. 7. According to this model, formation probabilities of $^4_\Lambda H$ hyperfragments are higher for higher energy Λ hyperons. The momentum transferred to the produced Λ hyperon with K^- at rest is about 250 MeV/c.   Therefore, one can expect that about the same or even more abundant hyperfragments must be produced in the electromagnetic production of a Λ hyperon, where the momentum transfer to the Λ hyperon is in the range of 250-450 MeV/c for photons in the energy range of 1-2 GeV.

The formation probability of $^4_\Lambda H$ from K^- absorption at rest on light nuclear targets was also investigated by employing anti-symmetrized molecular dynamics (AMD) combined with multi-step binary statistical decay [35]. The calculated hyperfragment isotope distribution of

a ^{12}C target is shown in Fig. 8. The total probability of *excited* hyperfragment formation amounts to about 29%. Mass distribution of $A \leq 10$ hyperfragments produced in AMD is about one-third of the total yield of the hyperfragments and the rest is the contribution of hyperon compound nuclei with mass number $A = 11$ and 12. Calculated result shows good agreement with the data of $^{4}_{\Lambda}H$ formation ($\sim 1\%$).

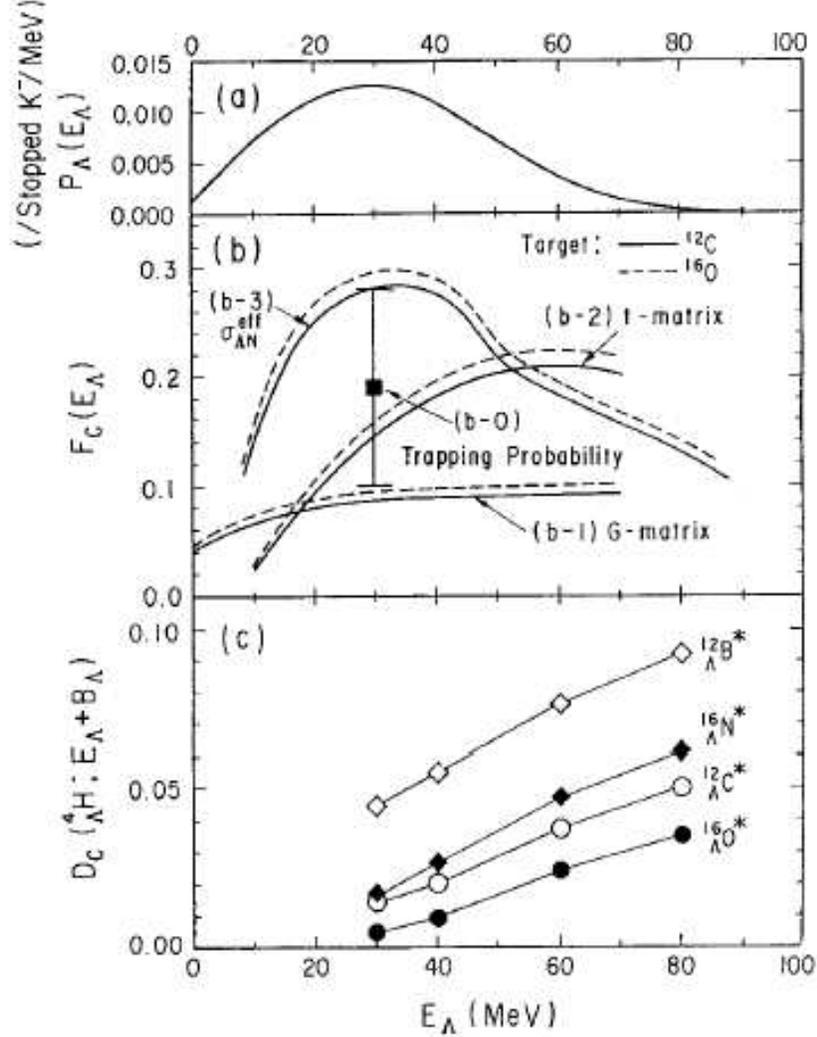Figure 7: (a) The calculated energy distribution of Λ produced from K^- absorption at rest. (b) The formation probabilities of the Λ compound nucleus on C and O targets, $F_c(E_\Lambda)$, estimated in four different ways, from the experimental hyperon trapping probability (b-0), from the imaginary part of the Λ potential calculated by the G-matrix (b-1) and by the t-matrix (b-2), and estimated by Yazaki from the ΛN cross section with the Pauli suppression effect (b-3). (c) The fragmentation probabilities of $^{4}_{\Lambda}H$ from the Λ compound nucleus, D_C ($^{4}_{\Lambda}H$, $E_X = E_\Lambda + B_\Lambda$) calculated for $^{12}_{\Lambda}C^*$, $^{12}_{\Lambda}B^*$, $^{16}_{\Lambda}O^*$ and $^{16}_{\Lambda}N^*$ (taken from Ref. [34]).
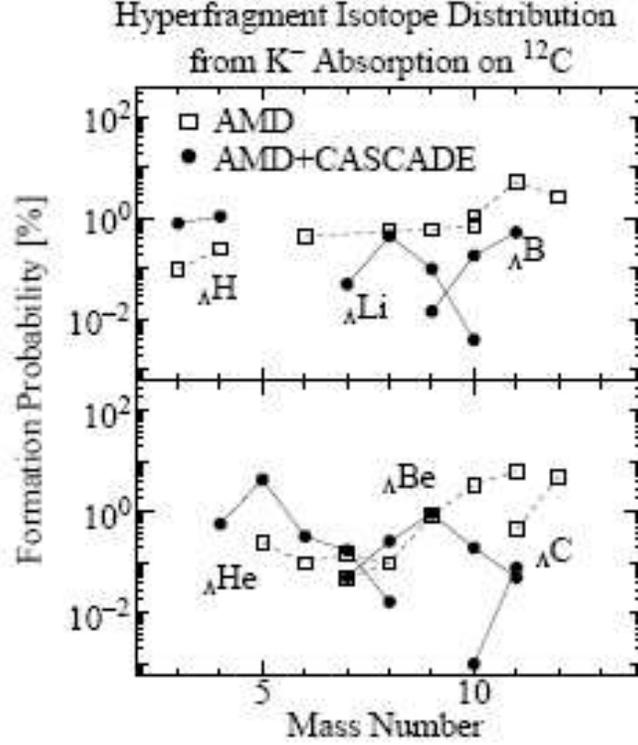
Figure 8: Hyperfragment isotope distribution from K^- absorption at rest on ^{12}C (from [35]). Boxes are the results of AMD calculation and black circles are the results after the multi-step statistical decay calculation.

These investigations demonstrate that as the target mass number decreases from ^{16}O, ^{12}C to ^9Be, the main formation mechanism varies from statistical decay, followed by dynamical fragmentation, to direct formation in the nuclear environment. As a result different excited parent hyperfragments are produced. To clarify the formation mechanism of $^4_\Lambda H$, it is worthwhile, following Nara [35] to examine the parent hyperfragment distribution of $^4_\Lambda H$ in the statistical decay. In Fig. 9, we show the parent hyperfragment distribution of $^4_\Lambda H$. We note from Fig. 9 that the sources of $^4_\Lambda H$ are dynamically produced neutron rich hyperfragments, and their mass numbers widely range from 6 to 12. This result gives a slightly different picture from the *hyperon compound nucleus* proposed in Ref. [34]. In Tamura's work, the sources of $^4_\Lambda H$ are limited to hyperon compound nuclei with mass number 11 and 12, and they have estimated the formation probability of $^4_\Lambda H$ to be about 0.24~0.67%. In this work, although the contribution from these hyperon compound nuclei amounts to about 0.6%, it is found that hyperfragments with $A \leq 10$ make non negligible contributions to the formation rates of $^4_\Lambda H$ (~0.5%), and their sum becomes the total yield (~1%). Thus the dynamical fragmentation or nucleon emission in the primary stage due to multi-step processes is indispensable for quantitative arguments, which means that due to this mechanism various exotic hypernuclei can be produced as hyperfragments that are impossible to produce by direct population.
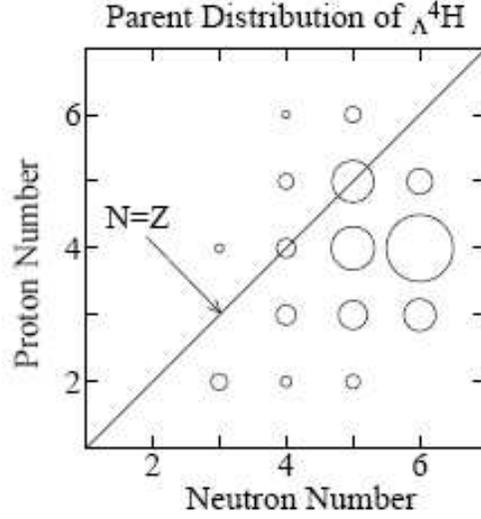
Figure 9: Parent hyperfragment distribution of $_\Lambda^4 H$ from K^- absorption at rest on ^{12}C. The area of the circle is proportional to the probability from that hyperfragment (from [35]).

The kinematics of strangeness production processes in case of photon interactions (Table 9) are very similar to K^- induced reactions at rest, especially for photons in the 2 GeV energy range.

Table 9: Two body reactions that photon produce strangeness (Λ hyperon).

1	$\gamma + p \rightarrow \Lambda + K^+$	4	$\gamma + n \rightarrow \Lambda + K^0$
2	$\gamma + p \rightarrow \Sigma^0 + K^+$	5	$\gamma + n \rightarrow \Sigma^- + K^+$
3	$\gamma + p \rightarrow \Sigma^+ + K^0$	6	$\gamma + n \rightarrow \Sigma^0 + K^0$

All these 6 reactions are potential sources of the hyperfragment formation. The hyperfragment formation cross section in case of K^- photo-production can be expressed as:

$$d\sigma(\gamma + A \rightarrow hyperfragment + K^+ + X)/d\Omega = A^{0.8} \times d\sigma(\gamma + N \rightarrow \Lambda(\Sigma) + K^+)/d\Omega \times \varepsilon_\Lambda \times \varepsilon_{hyp}^i,$$

where $d\sigma(\gamma + N \rightarrow \Lambda(\Sigma) + K^+)/d\Omega$ is the K^+ elementary photo-production cross section from nucleon and is equal to the sum of the cross sections of 1, 2 and 5 reactions in Table 9, ε_Λ is the Λ "sticking probability", and ε_{hyp}^i is the i-th hyperfragment formation weight. Here, for crude estimation, we assume $d\sigma(0°, \gamma + N \rightarrow \Lambda(\Sigma) + K^+)/d\Omega \approx 1$ $\mu b/sr$, with $\varepsilon_\Lambda = 0.20$, and for ε_{hyp}^i we take the same weights which have been observed in emulsion (Table 2). For the K^+ photo-production cross section on ^{12}C we have:

$$d\sigma(0°, \gamma + A \to K^+ + X)/d\Omega = A^{0.8} \times d\sigma(\gamma + N \to \Lambda(\Sigma) + K)/d\Omega \cong 4.2 \ \mu\text{b/sr}.$$

The indirect hyperfragment photoproduction cross section on ^{12}C can be then defined as:

$$d\sigma(\gamma + A \to hyperfragment + K^+ + X)/d\Omega \cong 4.2 \times \varepsilon_\Lambda \times \varepsilon_{hyp}^i \ \mu\text{b/sr}.$$

The resulting cross sections for the most probable hyperfragments are shown in Table 11. In addition to hyperfragment photo-production cross sections, relative weights of hyperfragments observed in emulsion, and available experimental [1] and theoretical [13] values for π^--decay widths are listed in Table 11 as well.

Table 11: Photo-production cross sections of light hyperfragments on ^{12}C target. In addition the relative weights and π^--decay widths are presented.

Hypernuclide	Photoproduction cross section (nb/sr)	Relative weight	π^--decay width $\Gamma_{\pi^-}/\Gamma_\Lambda$
$^3_\Lambda H$	42	0.05	0.3
$^4_\Lambda H$	33.6	0.04	0.5
$^5_\Lambda He$	420	0.45	0.34
$^7_\Lambda Li$	50.4	0.056	0.304
$^8_\Lambda Li$	165.5	0.197	0.368
$^8_\Lambda Be$	14.3	0.017	0.149
$^9_\Lambda Be$	46.2	0.055	0.172
$^{10}_\Lambda B$	2.1	0.0025	0.215
$^{11}_\Lambda B$	15.1	0.018	0.213
$^{12}_\Lambda B$ direct production	170	0.03	0.286

The Fig. 10 taken from Majling [36] shows clearly why the highly excited states of $^7_\Lambda He^*$ in which the "inner proton" is substituted by Λ ($Ps \to \Lambda$ transition) by means of $^7Li(\gamma, K^+)^7_\Lambda He^*$ reaction are the source of hyperfragments $^4_\Lambda H$ and $^6_\Lambda H$. The thresholds for these decay channels are rather high, but large changes in the structure of these states prevent the neutron or Λ emission.

The probability of a compound residual hot hypernuclear formation at the end of pre-equilibrium phase of high-energy photo-nuclear reactions was calculated recently [37] with a time dependent Monte Carlo Multi-collisional Cascade (MCMC) approach. The obtained results for the probabilities (Fig. 11), mass and charge distributions (Fig. 12) of the formed hot hypernucleus, demonstrate that the γ-nucleus interactions in the 1 GeV energy region is a rich source of Λ hyperfragments.
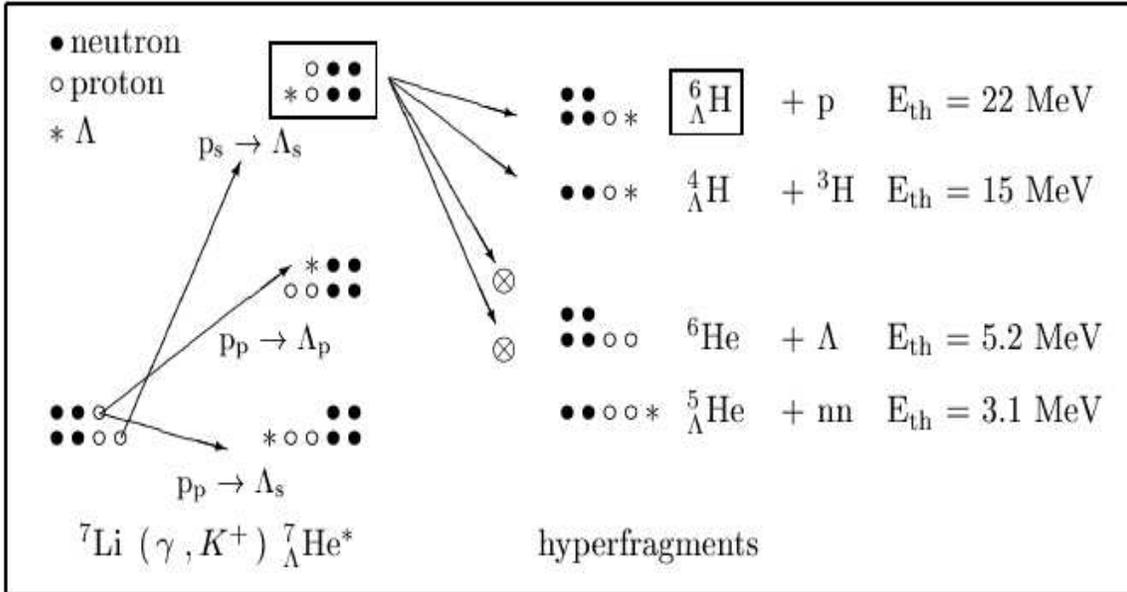
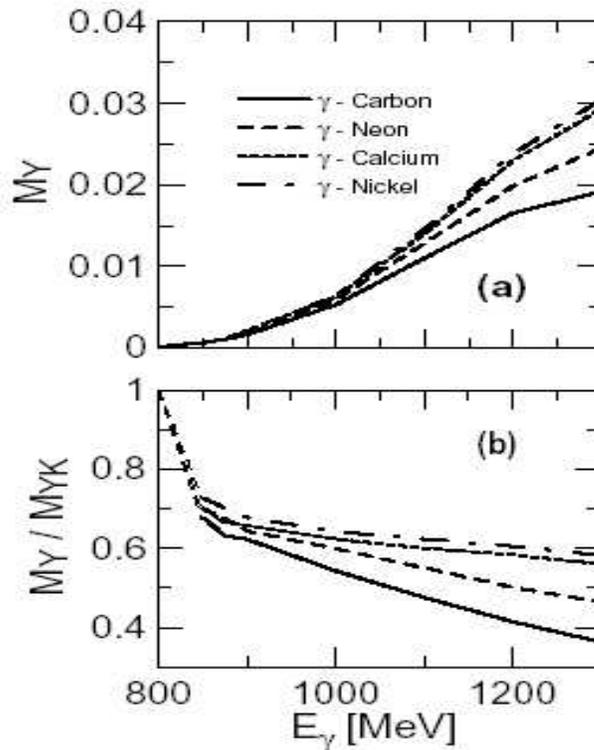Figure 10: Different decay channels of excited $^{7}_{\Lambda}He^{*}$ hypernucleus.

Figure 11: Hypernucleus multiplicity (a) and $M_Y/M_{YK}+$ ratio (b) as functions of incident photon energy for $^{12}C(\gamma, K^+)$ (solid lines), $^{20}Ne(\gamma, K^+)$ (dashed lines), $^{40}Ca(\gamma, K^+)$ (dotted lines), and $^{58}Ni(\gamma, K^+)$ (dot-dashed lines) reactions (from [37]). In (b) the short dashed lines linking the curves to the vertical axis do not result from calculation (see [37] for more details).
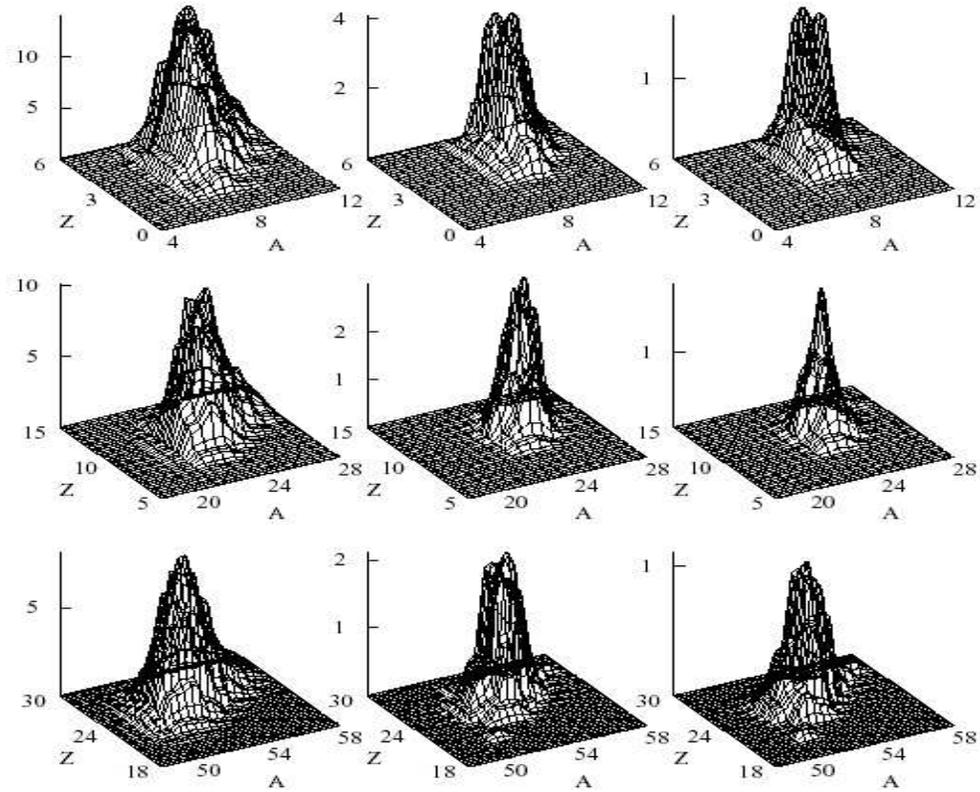
Figure 12: Residual nucleus mass and charge distributions for γ-Carbon (first row), γ-Aluminum (second row), and γ-Nickel (last row) at 1.2 GeV incident photon energy [37]. In the first column results for events inclusive in meson production (either a pion or a kaon) are displayed. In the middle column distributions of mass and charge considering only events with hyperon production in the primary interaction, however disregarding if the hyperon is kept bound or not, are shown. The last column is the distribution for events having a bound hyperon formed at the end of pre-equilibrium phase of the residual hot nucleus. The results in columns are multiplied, respectively, by 10^2, 2×10^4, and 2×10^4.

The large momentum transfer of the (π^+, K^+) reaction, which has been intensively used for production of hypernuclel recently, makes the quasi-free (QF) process dominant in the highly excited region where a Λ is knocked out from a nucleus. Some fraction of Λ produced in this region, however, trapped in the nucleus to form a hypernucleus through a finite probability of the ΛN scattering in nuclei. By using (π^+, K^+) reaction on ^{12}C target it was experimentally demonstrated that light Λ hypernuclei are produced followed after ΛN scattering [38]. The obtained probabilities (~20% of QF Λ) for the hypernuclear formation, suggests that there is a rich source of Λ hypernuclei in the QF regions of the (π^+, K^+), stopped K^-, and (γ, K^+) reactions.

From these discussions we can conclude that K^+ detection in the γ-nuclear interactions can serve as an effective (~20%) tag for different hypernuclear productions, which can be used to perform hypernuclear studies, e.g. weak decay π^- spectroscopy of hypernuclei with electron beam.

5. Proposed Project

We propose a new experiment for investigation of Λ hypernuclei by using the pionic decay. The project aims to determine precisely the binding energies of light hypernuclei, investigate production of exotic hypernuclei, and study impurity nuclear physics and the medium effect of baryons.

These investigations will fully utilize the unique features of the CEBAF beam and the newly developed experimental equipment (the HKS and Enge systems) dedicated for hypernuclear physics, as listed in the introduction chapter. These features make possible for the highest ever resolution and precision in using decay π^- to access the rich physics that hypernuclei can offer. All the equipment exist and are ready. Two production targets ^{12}C and ^{7}Li will be used to produce wide range of hypernuclei at ground states (or possible low lying states). We propose to run it in Hall C but it can be run in Hall A also by moving all the equipment to Hall A.

5.1 Experimental setup and expected performance

The experimental setup is rather similar to the HKS experiment (E01-011) completed in 2005. However, the beam lines will use the same design as that for the next experiment HKS-HES (E05-115) for easier beam handling. The general layout of the proposed experiment is illustrated in Fig. 13.
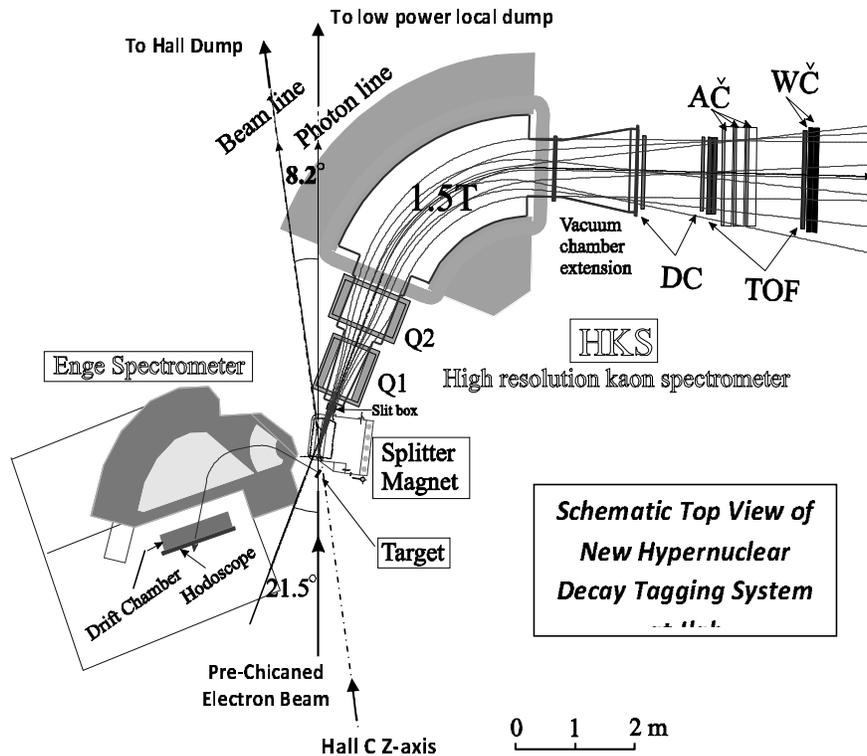

Figure 13: Schematic top view of the new hypernuclear decay tagging system.

The incident electron beam hits the target which will be moved upstream by ~15 cm with respect to the HKS normal target position to avoid decay pions experiencing the Splitter field. The 25 mg/cm^2 target will be tilted ~60° (30° incline to the beam). Thus, the effective target thickness will be about 50mg/cm^2. Positively charged kaons will be detected by HKS as usual. The precisely measured kaons with high momentum resolution provide efficient tagging in coincidence of decayed pions to exclude nuclear pions as well as the precisely reconstructed production time. They can also be used to reconstruct the recoil of extremely light hypernuclei for Doppler correction in case of decay in flight. The produced hypernuclei predominantly at forward direction are stopped in the target and decays after some 200 ps inside of the target. Decay pions have a discrete momentum lying in the range ≤133 MeV/c and exit the target. For the measurements of momentum and outgoing angles of these monochromatic pions, we will use the existing Enge spectrometer as the high-resolution pion spectrometer ($H\pi S$). The central optical axis of Enge will be normal to the target plane so that the target straggling energy loss uncertainty of the decayed pions will be minimized.

5.2 High-resolution pion spectrometer - $H\pi S$

For the measurement of decay pions in the 100 MeV/c regions, we will use the existing Enge Split-Pole spectrometer and its detector package that were used in both the HNSS/E89-009 and HKS/E01-011 experiments to detect low energy scattered electrons. A new additional Lucite Čerenkov counter can be used in anti-coincidence with the Enge timing hodoscope to veto electrons ($\beta = 1$) from the trigger of pions ($\beta \approx 0.72$).

A Monte-Carlo simulation was carried out to determine its acceptance and resolution and to optimize the spectrometer setup. The optical features and acceptance of the spectrometer are studied by the RAYTRACE simulation. The optical model of Enge spectrometer used in the RAYTRACE simulation was based upon the data card from the HNSS/E89-009 experiment, in which the parameters have been tuned to reproduce the realistic acceptance of the experimental data. A GEANT Monte-Carlo simulation was used to study effects of multiple scattering and energy loss from target, as well as detector widows and materials. The expected parameters are summarized in Table 12.

Table 12: Parameters of the $H\pi S$ spectrometer

Configuration	Enge Split-Pole spectrometer and detector package
Central momentum	115 MeV/c
Momentum acceptance	±40 %
Momentum resolution (r.m.s.)	10^{-4} without multiple scattering
Momentum resolution (r.m.s.)	4.9×10^{-4} with multiple scattering
Dispersion	1.28 cm/%
Time-zero precision	< 100 ps
Pion detection angle	~30 degree relative to the incident beam
Flight path length	309 c m
π^- survival rate	~ 60%
Solid angle	~20 msr
Total efficiency of the detector package	~80%

5.3 Momentum loss in the target

The energy resolution and the precision in determining the binding energies of hypernuclei are solely determined by the resolution and precision in analyzing the decayed pions. Due to ionization energy loss the monochromatic spectrum of decayed pions from a specific hypernuclear state is shifted as well as broadened. This is one of the two major sources contributed to the precision. Therefore the target thickness is selected to be thin enough to minimize target straggling effect to the decay pion spectra.

We have generated decay pion events and carried out a simulation study of decay pion spectra of hypernuclides by using the Monte Carlo method. The influence of the ionization energy loss has been calculated by using dedicated Monte Carlo code based on the individual collision method [39].

The dE/dx spectra of monochromatic pions (p = 115.8 MeV/c) from $^{12}_\Lambda B \rightarrow {}^{12}C + \pi^-$ decay passing through a 25 mg/cm^2 carbon target and the broadened momentum distribution are shown in Fig. 13a and Fig. 13b, respectively.
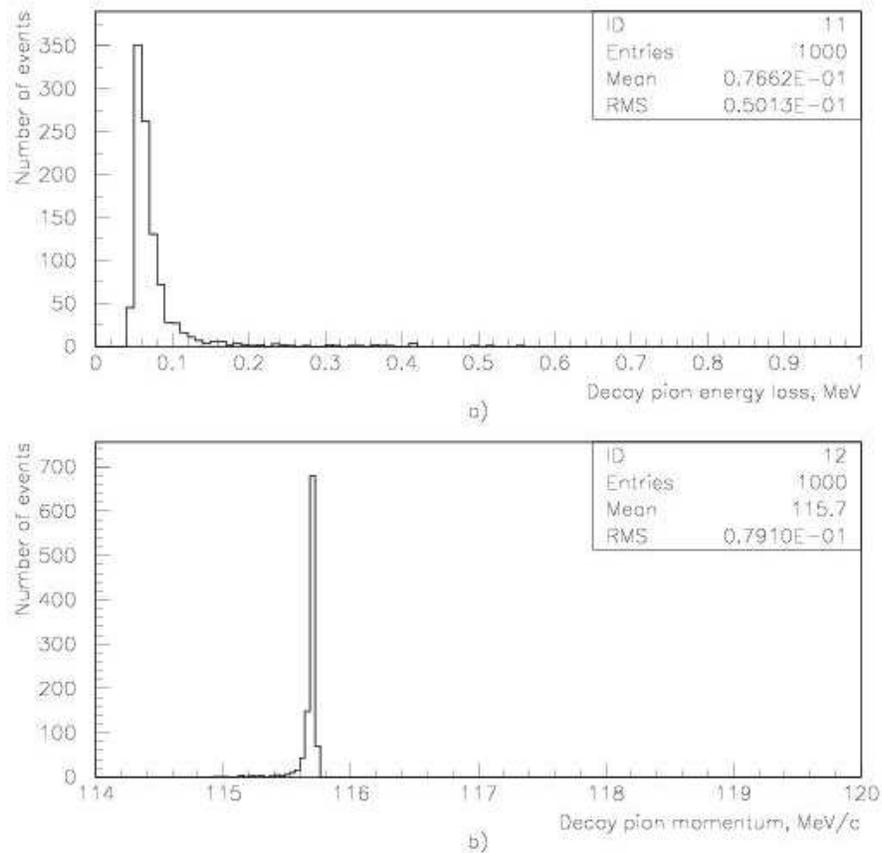

Figure 13: Simulated energy loss (a) and momentum (b) spectra of 115.8 MeV/c pions after passing through a 25 mg/cm^2 carbon target.

Similar results obtained in the case of pions randomly generated in the thickness of a 25 mg/cm^2 carbon target are shown in Fig. 14. Fig. 14a shows that the average energy loss is about 40 keV which will introduce the binding energy shift and the energy broadening is also about 40 keV which contributes to the energy resolution. Fig. 14b shows the effect from the energy shift and broadening to the pion momentum. The corresponding momentum shift is about 100 keV/c while the contribution to the momentum reolusion id about 70 keV/c. These pions were further transported to the focal plane of the Enge spectrometer. With the position resolution achieved by the existing detector system and the multiple scattering from the existing detector materials, the momentum resolution of $H\pi S$(Enge) is about 4.9×10^{-4} rms. Fig. 14c shows the overall result from a combined simulation that includes target straggling and focal plane detection errors and multiple scatterings. The overall momentum resolution is $\sigma = 92$ keV/c, corresponding to a binding energy resolution of $\sigma \approx 55$ keV. These simulations have been confirmed also by other independent GEANT simulation. Such energy resolution is capable to isolate structures separated by 120 keV or larger, such as the ground state doublet (1$^-$ and 2$^-$) of $^{12}_{\Lambda}$B.
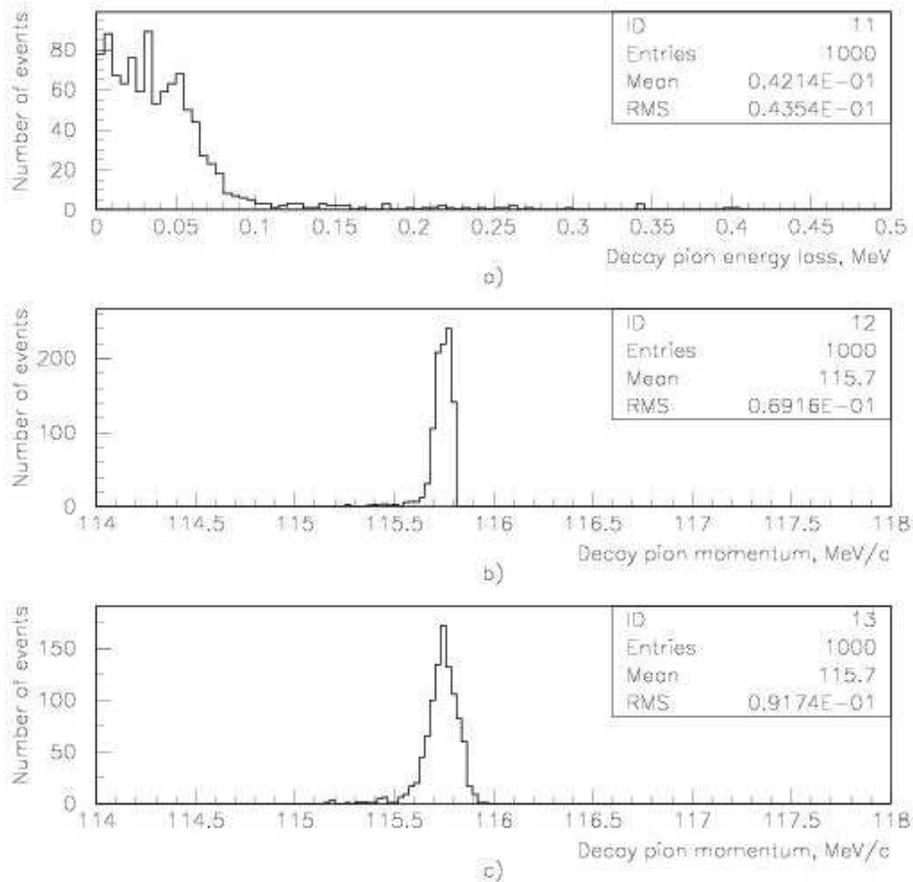

Figure 14: Simulated energy loss (a) and momentum (b) spectra for 115.8 MeV/c pions produced uniformly in the 25 mg/cm^2 carbon target; (c) is the momentum spectrum measured in the $H\pi S$ with resolution $\sigma = 4.9 \times 10^{-4}$.

The binding energy determination precision $\leq \pm 10$ keV will be achieved by two independent methods. The first method is a GEANT target energy loss simulation to extract the mean energy correction as a function of pion momentum. The second is the calibration using the monochromatic pions from decays of Λ produced by $\gamma p \to \Lambda K^+$ reaction. Water target can be used. The Doppler broadening to the pion momenta due to Λ recoil can be corrected by the kinematics reconstruction from the precise K^+ momentum and scattering angle reconstructions done by HKS. The mean of the "Λ" peak in terms of pion momentum will provide an absolute energy and momentum calibration in combination with the GEANT calculation of the target effect.

In addition, a δ scan by changing the Enge field setting can put the "Λ" peak at various momentum values across the focal plane. This in combination with Sieve Slit data will be used to calibrate the optics of $H\pi S$.

5.3 Expected yield of hypernuclei

The forward produced K^+ mesons detected in the HKS are a good trigger for hypernuclei production: about 3% of them are associated with "direct" and 20% with "indirect" production of hypernuclei. The remaining 77% of kaons are associated with quasi-free produced Λ particles, 64% of which decay through the $\Lambda \to \pi^- + p$ channel. The produced hypernuclei, besides light ($^3_\Lambda H$, $^4_\Lambda H$) ones, will stop in the target and decay after some 200ps with corresponding decay widths. The π^- decay widths for light hypernuclei ($A \leq 12$) lie in the range 0.15-0.5 (Table 11), e. g. the π^- decay width of the $^{12}_\Lambda B$ hypernucleus, which is produced directly through the $\gamma + ^{12}C \to ^{12}_\Lambda B + K^+$ reaction, is expected to be 0.286 [13]. Therefore, the π^- decay rate of $^{12}_\Lambda B$ from direct photo-production is expected to be:

$$R_{\pi^-}(^{12}_\Lambda B) = 0.03 \times 0.286 \times R_K = 0.0086 \times R_K ,$$

where R_K is the kaon single rate. For the "indirectly" produced hyperfragments, the corresponding π^- decay rates are determined as:

$$R^i_{\pi^-} = 0.2 \times \varepsilon^i_{hyp} \times \Gamma^i_{\pi^-} \times R_K ,$$

where ε^i_{hyp} and $\Gamma^i_{\pi^-}$ are population weights of hypernuclear isotopes and their π^- decay widths, respectively (see Table 11). The π^- decay rate from the quasi-free produced Λ particles is determined as:

$$R_{\pi^-}(\Lambda_{q.f.}) = 0.77 \times 0.64 \times R_K \cong 0.5 \times R_K .$$

Taking into account direct and indirect production mechanisms we can estimate the hyperfragment yields. The total π^- rate detected in the $H\pi S$ in coincidence with HKS is then:

$$R_{\pi^-}(H\pi S) = [\Delta\Omega/(4\times\pi)] \times \varepsilon_s \times \varepsilon^t_{eff} \times [R_{\pi^-}(^{12}_\Lambda B) + \sum_i R^i_{\pi^-} + R_\pi(\Lambda_{q.f.})] \times R_K ,$$

where $\Delta\Omega \approx 20$ *msr*, $\varepsilon_s \approx 0.6$, and $\varepsilon^t_{eff} \approx 0.8$ are the solid angular acceptance of $H\pi S$ (Enge), survival rate of the decayed pions, and total efficiency of the Enge spectrometer detector package, respectively. Thus alone the decay pion detection efficiency in $H\pi S$ is:

$$\varepsilon^{H\pi S}_{eff} = [\Delta\Omega/(4\times\pi)]\times\varepsilon_s \times \varepsilon^t_{eff} = 0.88\times10^{-3}.$$

The hypernuclear decay pion "daily" yields detected in $H\pi S$ in the case of 150 Hz K^+ rate in HKS for ^{12}C target (i.e. scaled from the E01-011 condition: $45\mu A$ beam and 50mg/cm^2 target) are listed in Table 13. For $^{12}_\Lambda B$ we consider only the direct production mechanism. In Table 13, the relative weights evaluated from emulsion data and the decay pion yield from quasi-free produced Λ are listed as well. The corresponding discrete pion spectrum detected in $H\pi S$ without background is illustrated in Fig. 15.

Table 13: Hypernuclei (ground states only) and decay pion "daily" yields for ^{12}C target (t_{eff} = 50 mg/cm^2) with 150 Hz K^+ rate in HKS (Beam current: $45\mu A$).

Hypernuclei	Relative yield	π^--decay width $\Gamma_{\pi^-}/\Gamma_\Lambda$	Decay π^- "daily" yield detected in $H\pi S$	π^- Mom. (MeV/c)
q. f. Λ	0.77	0.64	8.6×10^3	
$^3_\Lambda H$	0.01	0.30	23	114.3
$^4_\Lambda H$	0.01	0.50	31	132.9
$^5_\Lambda He$	0.09	0.34	239	99.14
$^7_\Lambda Li$	0.01	0.30	27	107.9
$^8_\Lambda Li$	0.04	0.37	113	124.1
$^8_\Lambda Be$	0.004	0.15	4	97.17
$^9_\Lambda Be$	0.01	0.17	15	95.96
$^{11}_\Lambda B$	0.004	0.21	6	105.9
$^{12}_\Lambda B$ - direct production	0.03	0.29	134	115.8

It is worthwhile to mention that the expected spectrum of hyperfragments will be different than the demonstrated one (see the last column of Fig.12). This is connected to the fact that for identification purposes, in emulsion, events decaying into more than two particles were mainly considered. In this experiment the two body decay events will be detected. So the presented hyperfragment spectrum only demonstrates the sensitivity of the proposed experiment and its expected resolution. Background was not included and will be discussed below. In addition, no low lying states were considered in this illustration since their yields depend on the production cross sections and decay widths, thus varying case by case.
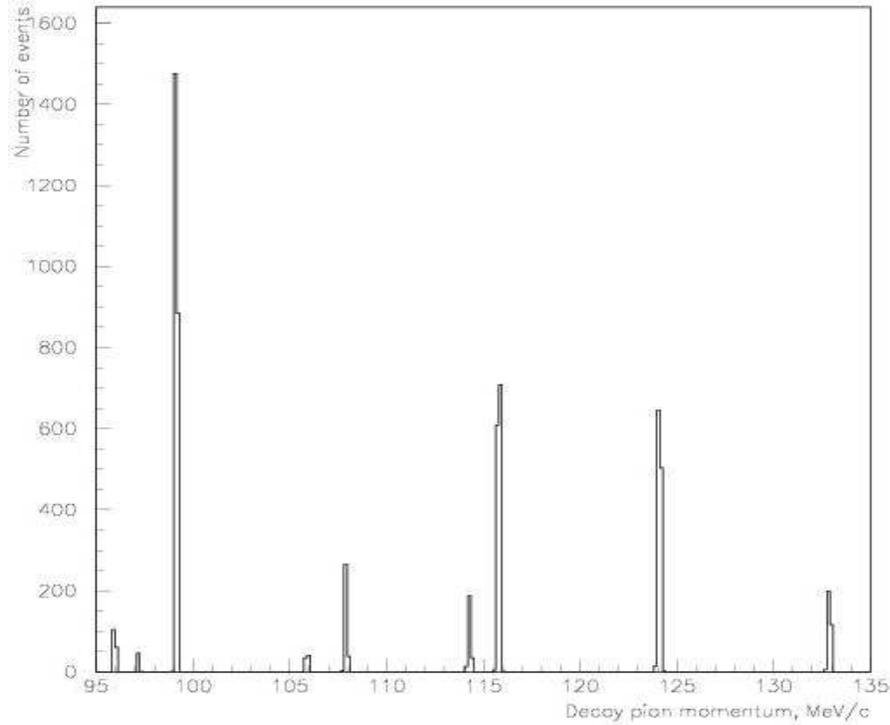
Figure 15: Demonstration of π^- decay spectra from different hyperfragments with their relative weights evaluated from emulsion data; the target straggling is taken into account with target thickness of 25 mg/cm^2; the $H\pi S$ resolution is $\sigma = 4.9 \times 10^{-4}$; and total number of events is 6000.

5.4 Background

In the real experimental conditions, we will have three sources of background:
a) The promptly produced pions;
b) The decay pions from quasi-free produced Λ particles;
c) Accidentals.
The promptly produced pions will be excluded by using coincidence requirement with the produced kaons. With tight 2ns coincidence window gate, all of them will be eliminated. However, this way does not allow excluding background from the decay of quasi-free produced Λ particles or from accidental coincidences. We carried out simulation studies of the decay pion spectrum from quasi-free produced Λ particles by using the Monte Carlo method. We took into account the following factors for the final distribution:

1. The momentum distribution of the "quasi-free" produced Λ particles. We assume isotropic production for the C.M. angular distribution with Gaussian momentum distribution (mean value is 200 MeV/c and $\sigma = 100$ MeV/c);
2. The full π^- spectrum are: 88% pions from "quasi-free" produced Λ particles, and 12% monochromatic pions from different hyperfragments with their relative weights, evaluated from the last column of Table 13;
3. The momentum resolution of the pion spectrometer; and
4. The ionization energy loss.

The simulated spectrum including background with total of 10^5 pions produced in the 25 mg/cm^2 carbon target (with energy loss) and measured in the $H\pi S$ with resolution $\sigma = 4.9 \times 10^{-4}$ is shown in Fig. 16. It demonstrates that monochromatic pion spectra are clearly seen even with a huge amount of quasi-free background.
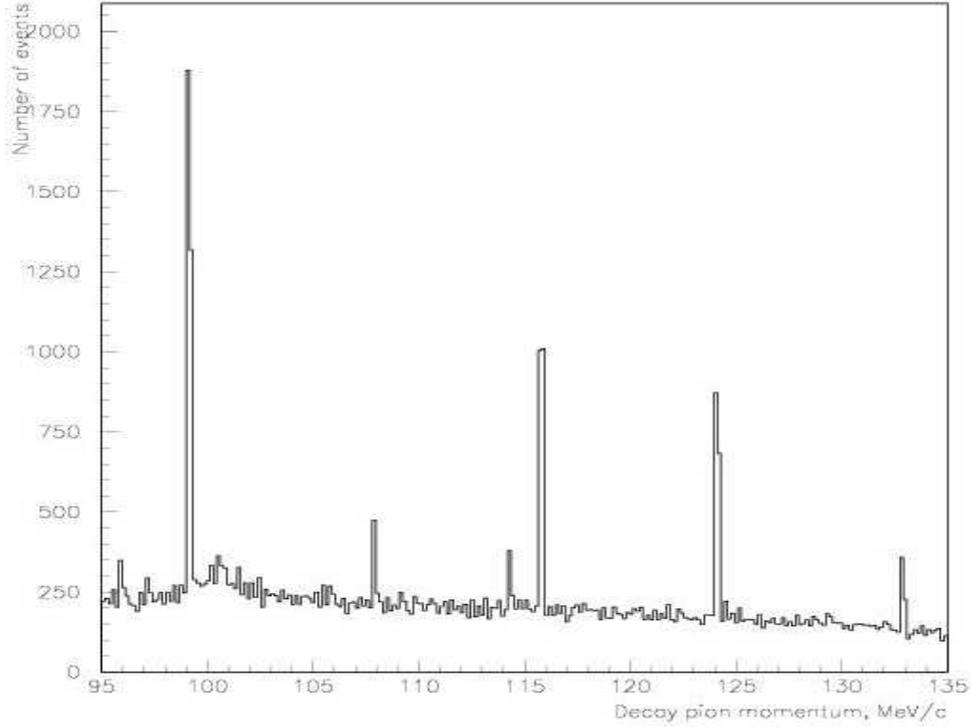

Figure 16: Simulated spectrum of the decayed pions (93.5% from quasi-free produced Λ particles, and 6.5% from different hyperfragments with their relative weights). Target thickness is 25 mg/cm^2; momentum resolution of $H\pi S$ is $\sigma = 4.9 \times 10^{-4}$; and total number of events is 10^5.

5.5 Accidentals

The typical rate of kaons detected in HKS is about 200 count/s (with 30 μA beam current and a 100 mg/cm^2 C target). The simulations from the Radiation Control group (Pavel Degtiarenko) for a 30% momentum acceptance and 30 msr solid angle for the pion spectrometer show a 1.4×10^3/s rate for negatively charged pions. This implies an accidental rate of 5.6×10^{-4}/s within a 2 ns time window. In the 100 keV/c momentum bites in which the discrete pions are localized, this rate will be about 2×10^{-6}/s, which is negligible.

5.6 Requested Beam Time

In the proposed experiment we intend to measure precisely the decay pion spectra of light hypernuclei which are produced in electron nuclear interactions "directly" or "indirectly". Our main goal is to measure precisely the binding energies, of $^3_\Lambda H$, $^4_\Lambda H$, $^7_\Lambda He$,

$^{12}_{\Lambda}B$ hypernuclei and other hyperfragments which will show up in $H\pi S$ with sufficient statistical significance. We propose to use two production targets: ^{7}Li, and ^{12}C. It is expected that by decreasing the target mass, the production rates of $^{3}_{\Lambda}H$ and $^{4}_{\Lambda}H$ are increased. Also for the ^{7}Li target we are expecting formation of exotic $^{6}_{\Lambda}H$ hyperfragment (see Fig. 10 and reference [36]).

We ask 20 days of beam time for each production target. The requested data taking hours were calculated so that at least about 1000 counts for $^{3}_{\Lambda}H$ and $^{4}_{\Lambda}H$ each can be accumulated and it makes possible for hypernuclei with three times smaller yield to show up with sufficient statistics. Thus, the total required data acquisition time is 40 days. In addition, we require 2 weeks commissioning to setup and calibrate the two spectrometer systems.

6 Summary

High resolution decay pion spectroscopy for light hypernuclei is proposed. The main goal of the present proposal postulates that we use the high resolution kaon spectrometer (HKS) and high resolution Enge spectrometer as the pion spectrometer ($H\pi S$) to carry out decay pion spectroscopy from two light production targets ^{7}Li, and ^{12}C and measure precisely binding energies and lifetimes of produced light hypernuclei or hyperfragments at about 2 GeV electron beam. The proposal is based on the successful operation of these magnetic spectrometers in Hall C at JLab and will fully take the advantage of the CEBAF high-quality high-power CW electron beam.

The physics subjects which can be investigated by means of decay pion spectroscopy include: (1) YN interactions, (2) study of exotic hypernuclei, (3) impurity nuclear physics, and (4) medium effect of baryons. This will be the most precise experiment for measuring of binding energies of light hypernuclei.

The proposed experimental program is a unique one and is not duplicated by any in the currently approved or planned experimental programs and can be performed only with the CEABF electron beam.

References

1. D. H. Davis, "50 years of hypernuclear physics, I. The early experiments", Nucl. Phys. A 754 (2005) 3c.
2. R. H. Dalitz, "50 years of hypernuclear physics, II. The later years", Nucl. Phys. A 754 (2005) 14c.
3. G. Keyes, M. Derrick, T. Fields et al., "Properties of the hypertriton", Phys. Rev. D1, 66 (1970).
4. A. Margaryan, O. Hashimoto, S. Majewski, L. Tang "RF Cherenkov picosecond timing technique for Jlab 12 GeV physics program" LOI to this PAC.

5. O. Hashimoto, L. Tang, J. Reinhold (spokespersons), "Spectroscopic study of Λ hypernuclei up to medium-heavy mass region through the in the (e, e'K$^+$) reaction", JLAB Experiment E01-011.

6. O. Hashimoto, S. Nakamura, L. Tang, J. Reinhold "Spectroscopic investigation of Λ hypernuclei in the wide mass region using the (e, e'K$^+$) reaction", JLAB Experiment E05-115.

7. J-PARC Strangeness Nuclear Physics Group, Letter of intent for "New generation spectroscopy of hadron many body systems with strangeness S=-2 and -1", Letter of intent for nuclear and particle physics experiments at the J-PARC, J-PARC 03-6.

8. O. Hashimoto, H. Tamura, "Spectroscopy of Λ hypernuclei", Progress in Particle and Nuclear Physics 57 (2006) 564-653.

9. Th. Rijken, Y. Yamamoto, "Recent soft-core baryon-baryon interactions", Nucl. Phys. A 754 (2005) 27c.

10. A. Nogga, "Faddeev-Yakubovski calculations for A=4 hypernuclear system", Nucl. Phys. A 754 (2005) 36c.

11. Y. Fujimura, C. Nakamoto, M. Kohno, Y. Suzuki, K. Miyagawa, "Interactions between octet baryons and their applications to light hypernuclei", Nucl. Phys. A 754 (2005) 43c.

12. H. Nemura, Y. Akaishi, and Y. Suzuki, "Ab initio Approach to s-Shell Hypernuclei $^3_\Lambda H$, $^4_\Lambda H$, $^4_\Lambda He$, and $^5_\Lambda He$ with a $\Lambda N - \Sigma N$ Interaction", Phys. Rev. Lett. 89 (2002) 142504-1.

13. T. Motoba and K. Itonaga, "Pi-Mesonic Weak Decay Rates of Light-to-Heavy Hypernuclei", Progress of Theoretical Physics Supplement, No. 117, (1994) p.477.

14. T. Motoba, "Mesonic weak decay of strange nuclear systems", Proceedings of the IV International Symposium on Weak and Electromagnetic Interactions in Nuclei, 12-16 June 1995, Osaka, Japan. Edited by H. Ejiri, T. Kishimoto and T. Sato, World Scientific, 1995, p.504.

15. E. Hiyama, M. Kamimura, T. Motoba, T. Yamada, Y. Yamamoto, "Three-body model study of $A = 6-7$ hypernuclei: Halo and skin structures", Phys. Rev. C53, (1996) 2075.

16. L. Majling et al., "Superheavy Hydrogen Hypernucleus $^6_\Lambda H$", AIP Conference Proceedings Volume 831, (2006)p. 493.

17. P. K. Saha, T. Fukuda and H. Noumi, "Neutron-reach hypernuclei by the double-charge exchange reaction", Letter of Intent for Nuclear and Particle Physics experiments at the J-PARC (LOI9), 2002.

18. E. Hiyama, M. Kamimura, K. Miyazaki, T. Motoba, "γ-transitions in A=7 hypernuclei and a possible derivation of hypernuclear size", Phys. Rev. C59 (1999)2351.

19. K. Tanida, H. Tamura, D. Abe et al., "Measurement of the B(E2) of $^7_\Lambda Li$ and Shrinkage of the Hypernuclear Size" Phys. Rev. Lett. 86 (2001) 1982.

20. H. Tamura, "High resolution spectroscopy of Λ hypernuclei: present status and perspectives", Nucl. Phys. A691 (2001) 86c. "Impurity nuclear physics: Hypernuclear γ spectroscopy and future plans for neutron-reach hypernuclei" The European Physical Journal A-Hadrons and Nuclei, V13 (2002) 181.

21. R. H. Dalitz and A. Gal "The formation of, and the γ-radiation from, the shell hypernuclei" Ann. Phys. 116 (1978) 167.

22. D. J. Millener, "Shell-model description of Λ hypernuclei", Nucl. Phys. A691 (2001) 93c.

23. M. Juric, G. Bohm, J. Klabuhn et al., "A new determination of the binding-energy values of the light hypernuclei (A $\leq$ 15)", Nucl. Phys. B 52 (1973) 1.

24. T. Yamazaki et al., "New aspects and new tools in hypernuclear studies: experiments with a superconducting toroidal spectrometer" INS-Rep.-728 (1988).

25. H. Outa et al., "Lifetime measurement of $^4_\Lambda H$ hypernucleus", INS-Rep.-914 (1992).

26. The FINUDA Collaboration, "FINUDA A DETECTOR FOR NUCLEAR PHYSICS AT DAΦNE, LNF-93/021 (1993).

27. F. X. Lee, T. Mart, C. Bennhold, H. Haberzettl, L. E. Wright, "Quasifree Kaon Photoproduction on Nuclei", arXiv: nucl-th/9907119.

28. H. Yamazaki et al., "The $^{12}C(\gamma, K^+)$ reaction in the threshold region", Phys. Rev. C 52, R1157–R1160 (1995).

29. M. Sotona et al., Proceedings of Mesons and Light Nuclei '98, (1998) 207.

30. T. Mart, D. Kusno, C. Bennhold, L. Tiator, D. Drechsel, "Photoproduction of the hypertriton", arXiv: nucl-th/9610038.

31. T. Mart, L. Tiator, D. Drechsel, C. Bennhold, "Electromagnetic production of the hypertriton", arXiv: nucl-th/9708012, Nucl. Phys. A640 (1998) 235.

32. F. Dohman et al., "Angular distributions for hyper He-3, He-4 bound states in the He-3, He-4(e, e-prime K+) reaction, Phys. Rev. Lett. V 93 (2004) 242501.

33. H. Tamura, T. Yamazaki, R. S. Hayano et al., "Formation of $^4_\Lambda H$ hypernuclei from K^- absorption at rest on light nuclei", Phys. Rev. C 40 (1989) R479.

34. H. Tamura, T. Yamazaki, M. Sano et al., "Compound-hypernucleus interpretation on $^4_\Lambda H$ formation probabilities in stopped- K^- absorption", Phys. Rev. C 40 (1989) R483.

35. Y. Nara, A. Ohnishi and T. Harada, "Target mass dependence of $^4_\Lambda H$ formation mechanism from K^- absorption at rest", *Phys. Lett.* 346 *(1995)* 217.

36. Lubomir Majling, "Hypernuclei $^6_\Lambda H$ and $^8_\Lambda H$ could be identified – so what?", IX International Conference on Hypernuclear and Strange Particle Physics, October 10-14, 2006, Mainz, Germany.

37. M. Goncalves, E.C. de Oliveira, E.L. Medeiros, S. de Pina, and S.B. Duarte, **"**Hot Hypernucleus Formation in High-Energy Photonuclear Reactions", Brazilian Journal of Physics, vol. 34, no. 3A, September, 2004, 919.

38. S. Ajimura et al., "Λ Hypernuclei by Quasifree (π^+, K^+) Reaction on ^{12}C", Nuclear Physics A577 (1994) 271c-276c.

39. K. A. Ispirian, A. T. Margarian, A. M. Zverev "A Monte Carlo method for calculation of the distribution of ionization losses"**,** Nucl. Instr. and Meth.117 (1974) 125.